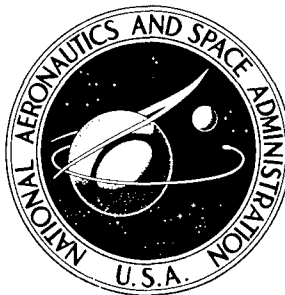


NASA TECHNICAL NOTE



~~100%~~
NASA TN D-4461

NASA TN D-4461

AMPTIAC

DISTRIBUTION STATEMENT A
Approved for Public Release
Distribution Unlimited

USE OF SURFACE REPLICATION,
EXTRACTION REPLICATION, AND
THIN-FILM ELECTRON MICROSCOPY
IN THE STUDY OF
DISPERSION-STRENGTHENED MATERIALS

by Charles A. Hoffman and Bruno C. Buzek

Lewis Research Center

Cleveland, Ohio

20060516223

USE OF SURFACE REPLICATION, EXTRACTION REPLICATION,
AND THIN-FILM ELECTRON MICROSCOPY IN THE STUDY OF
DISPERSION-STRENGTHENED MATERIALS

By Charles A. Hoffman and Bruno C. Buzek

Lewis Research Center
Cleveland, Ohio

NATIONAL AERONAUTICS AND SPACE ADMINISTRATION

For sale by the Clearinghouse for Federal Scientific and Technical Information
Springfield, Virginia 22151 - CFSTI price \$3.00

USE OF SURFACE REPLICATION, EXTRACTION REPLICATION, AND THIN-FILM ELECTRON MICROSCOPY IN THE STUDY OF DISPERSION-STRENGTHENED MATERIALS

by Charles A. Hoffman and Bruno C. Buzek

Lewis Research Center

SUMMARY

An investigation was conducted to obtain experimental indications of the relative merits of surface replication, extraction replication, and thin-film methods as currently used at Lewis to evaluate the microstructures of dispersion-strengthened materials. The conclusions of this study, based on two types of materials whose finest resolved particles were of the order of 100 \AA (0.01 \mu m), were as follows: surface replication gave the best agreement of measured and nominal amounts of oxide whether the oxide was discrete and spheroidal (i. e., nickel + thorium dioxide ($\text{Ni} + \text{ThO}_2$)) or plate-like and aggregated (i. e., aluminum + aluminum oxide ($\text{Al} + \text{Al}_2\text{O}_3$)); this method was also felt to give the most satisfactory value of average particle size ($\overline{\text{PS}}$) and average interparticle spacing ($\overline{\text{IPS}}$). Extraction replication was also satisfactory for the former material but not for the latter; the validity of the extraction method was dependent on the shape of the oxide particles and its state of aggregation as well as the effectiveness of the extraction technique. The thin-film method was helpful in verifying the existence of the finer particles but gave considerably greater volume fractions of oxide particles compared to the respective nominal amounts: For the $\text{Ni} + \text{ThO}_2$ the calculated $\overline{\text{IPS}}$ decreased, while for the $\text{Al} + \text{Al}_2\text{O}_3$ not even an apparent $\overline{\text{PS}}$ or $\overline{\text{IPS}}$ could be calculated because of particle aggregation and/or overlap. Particle-size - frequency distributions obtained from each of the three methods when applied to the $\text{Ni} + \text{ThO}_2$ essentially agreed. Stereoscopic, or three-dimensional, views of thin films gave better indication of the shape of the particles and the spatial relations between particles. Under some conditions, stereoscopic views can thus supplement and/or provide cross checks on surface or extraction replication.

end

INTRODUCTION

The potential benefits derived from the use of dispersion-strengthened materials are

well known. Theory and experiments have shown that the properties of these materials are related to the average interparticle spacing \overline{IPS} ; this in turn is related to the average particle size \overline{PS} and the volume percent of the dispersoid. The effect of particle size per se on strength is not well defined, but a study of several of the best dispersion-strengthened materials (ref. 1) indicates that a desirable \overline{PS} is probably 0.05 micron ($0.05 \mu\text{m}$) or less. In addition, particle shape (refs. 2 to 4) and uniformity of dispersion probably influence mechanical properties. The microstructural factors discussed previously - \overline{IPS} , \overline{PS} , volume percent, shape, and uniformity - must be determined with reasonable accuracy to characterize any given dispersion-strengthened material meaningfully. Only metallographic techniques can be used to define the in-situ \overline{IPS} , shape, and uniformity, as well as volume percent and \overline{PS} . Because of the fine particle sizes involved (considerably less than $1 \mu\text{m}$), it is necessary to use electron microscopy to resolve particles.

Currently, there are three principal electron microscopy methods being used: (1) surface replication, (2) extraction replication, and (3) thin-film techniques. Each of these methods has certain a priori advantages and disadvantages. Surface replication has the advantage of ease of preparation, indicates overall morphology, and appears to give accurate characterizations when using available analytical methods based on topological measurements. The disadvantages are that it requires (1) a flat surface, (2) an optimal amount of etching, and (3) an optimal amount of shadowing. The extraction replication technique should delineate the particles better, produce a result free of matrix effects, and be amenable to topological analysis. Conversely, fine particles might be dissolved, some particles might float away, particles may shift from their initial positions, and removal of particles from subsurface layers would give an apparent larger volume percentage and \overline{PS} and a smaller \overline{IPS} . The thin-film method would delineate fine particles and when applied stereoscopically would give good qualitative indications of particle shape and spatial distribution. But the third dimension would make quantitative analysis difficult. Partially densified material especially would be unsuited to this method.

This study seeks to ascertain, experimentally, the relative merits of surface replication, extraction replication, and thin-film techniques (including three-dimensional viewing) as currently used at Lewis for characterizing dispersoids of different geometries and spatial relations. (That is, more insight relative to the choice of methods to characterize a given structure will thus be sought.) The materials selected were nominally aluminum plus 5-percent aluminum oxide ($\text{Al} + 5 \text{Al}_2\text{O}_3$) and nickel plus 2-percent thorium dioxide ($\text{Ni} + 2 \text{ThO}_2$). These materials contain dispersoids that differ widely in shape and spatial distribution, as will be apparent subsequently. To compare the values of volume percent, \overline{PS} , and \overline{IPS} for the two materials and the three electron-microscopy methods, lineal and area analyses - that is, topological methods (refs. 5

and 6) - were used. The application of topological methods would be expected to become increasingly inaccurate as the preparation techniques progress from planar to three-dimensional. Single representative transverse micrographs were studied for each material subjected to each electron-microscopy technique.

MATERIALS, APPARATUS, AND PROCEDURE

Materials

The materials investigated were Alcoa M-257 ($\text{Al} + 5 \text{Al}_2\text{O}_3$) and du Pont TD-nickel ($\text{Ni} + 2 \text{ThO}_2$), obtained in bar form. Chemical analyses performed on these materials indicated that the former contained about 4.2 volume percent Al_2O_3 and the latter about 1.8 volume percent ThO_2 . Specimens of each material examined were taken from the same rod and were within about 1 centimeter of each other.

Apparatus

A Phillips model 100B electron microscope with a practical resolution of about 20 Å ($0.002 \mu\text{m}$) was used. The specimen holder in the Phillips electron microscope could be tilted $\pm 10^\circ$, permitting the photographing of the same area of the specimen but from two slightly different angles, equally inclined about the electron beam axis. Stereoscopic viewing of two such matching photographs (i. e., the thin films) produce a three-dimensional effect. Thin-film electron photomicrographs were taken of each of the two materials, as well as photomicrographs of the surface and extraction replicas.

Procedure

Surface replication. - Transverse specimens of each of the materials were metallographically polished with 320 and 600 grit papers and final polished with number 3 and then number 1/2 diamond polish. The $\text{Al} + \text{Al}_2\text{O}_3$ was subsequently polished with magnesium oxide (MgO).

The specimens were etched with the indicated solutions:

Material	Solution
Al + Al ₂ O ₃	3 g NaOH 3 g Na ₂ CO ₃ 50 ml H ₂ O
Ni + ThO ₂	92 ml HCl 3 ml HNO ₃ 5 ml H ₂ SO ₄ 400 ml H ₂ O

The surfaces were then cleaned and a Mowital plastic layer was formed on each by dropping 0.25 percent Mowital in chloroform on it. The Mowital film was reinforced by a thin layer of Parlodion dissolved in amyl acetate. The combined layer was removed with cellulose adhesive tape. The replicated side of the plastic film was then shadowed with uranium dioxide (UO₂). The UO₂ layer was subsequently covered with an approximately 100-Å- (0.01-μm-) thick film of vapor-deposited carbon. Then the Mowital plus Parlodion was dissolved away leaving only the UO₂ shadowed carbon film.

Extraction replication. - The specimens used for this technique were prepared in the same metallographic fashion as those used for surface replication. These specimens were then coated with an approximately 200-Å- (0.02-μm) thick vapor-deposited film of carbon. The carbon film was scored and the specimen-film combination was placed in one dish containing 3 percent bromine in methanol for the Ni + ThO₂, and in another dish containing saturated mercuric chloride for the Al + Al₂O₃. Etching proceeded through the scored portion of the carbon backing; the matrices were dissolved leaving dispersoid particles attached to the carbon films. When the extraction was complete, the films floated free of the specimens. The extraction film containing the ThO₂ particles was washed several times in methyl alcohol; the film containing the Al₂O₃ particles was washed in dilute HCl followed by a wash in H₂O.

Thin films. - Disks about 1 centimeter in diameter and 0.2 centimeter thick were cut from a bar of each material. These disks were annealed at 600° C (872° K) for 4 hours in argon and rolled to a thickness of about 0.01 centimeter. The central portion of each disk was further reduced in thickness by peening. The disks were then reduced to a final maximum thickness of about 0.1 micron. This was accomplished by electropolishing the Ni + ThO₂, and by electropolishing and then chemical polishing the Al + Al₂O₃.

The polishing solutions used were as follows:

Material	Electro-polish solution	Chemical-polish solution
Ni + ThO ₂	45 cc H ₃ PO ₄ 30 cc H ₂ SO ₄ 25 cc H ₂ O	
Al + Al ₂ O ₃	10 cc HNO ₃ 90 cc H ₂ O 2.5 g CrO ₃	70 cc H ₃ PO ₄ 3 cc HNO ₃ 12 cc CH ₃ CO ₂ H (acetic acid) 15 cc H ₂ O

The electrolytic solutions were gently agitated to remove oxide particles that came off during electropolishing and to keep these particles suspended so that they would not settle back on the specimen surfaces.

Methods of calculating and comparing particle parameters. - Area and lineal analyses were used to obtain quantitative values for subsequent comparisons of the results obtained from the three electron microscopy methods. Analyses were made of electron photomicrographs which represented (1) a flat polished plane in the instance of the surface-replicated material, (2) a flat polished surface made irregular by dissolution of the matrix in the instance of the extraction-replicated material, and (3) a volume (i. e., a thin film probably at least several times as thick as the particles contained therein) in the case of the thin-film specimens.

Topological analysis of pseudo-surfaces (i. e., electron photomicrographs of thin-film, extraction, and/or overetched replication specimens) may lead to possible errors in characterizing particles existing in a volume of material, that is, in the calculation of volume percent, \overline{PS} , and \overline{IPS} . At present, there seems to be no two-dimensional measuring technique that can allow for a third dimension.

The method generally used at this laboratory for characterizing materials containing spheroidal dispersoids such as the Ni + ThO₂ is as follows. The area of each particle is determined by visually equating it to a reference area provided by a Zeiss particle size analyzer (ref. 1). The volume fraction of particles is obtained by area analysis and is taken as

$$\text{Volume percent} = \frac{A}{A_M}$$

where A is the total area of particles in field viewed and A_M the area of micrograph viewed. The \overline{IPS} and \overline{PS} are obtained from the following equations (see derivation in the appendix) in conjunction with area analysis:

$$\overline{\text{IPS}} = \frac{\pi A}{P} \left(\frac{1}{f_{\text{ox}}} - 1 \right) \quad (1)$$

$$\overline{\text{PS}} \equiv \overline{Z} = \frac{\pi A}{P} \quad (2)$$

where

- $\overline{\text{IPS}}$ average interparticle spacing in a three-dimensional array of particles
- A total particle area determined from a micrograph (assuming circular plane sections for particles)
- P total particle perimeter determined from a micrograph (assuming circular plane sections for particles)
- f_{ox} volume fraction of secondary phase particles (i. e. , total area of particles divided by total area viewed)
- $\overline{\text{PS}} \equiv \overline{Z}$ average particle intercept dimension defined as average intercepted length on randomly oriented straight lines through a random array of particles

The volume percent of dispersoid was determined for all the Al + Al₂O₃ specimens by use of lineal intercept measurements and the relation (from ref. 5)

$$\text{Volume percent} = \frac{La}{L}$$

where La is the total length of random traversing line(s) intercepted by the dispersoid phase, and L the total length of random traversing line(s) applied to field being viewed. The $\overline{\text{IPS}}$ and $\overline{\text{PS}}$ were determined for the surface replication specimen of Al + Al₂O₃ by the relations (refs. 5 and 6)

$$\overline{\text{IPS}} = 4 \left(\frac{V}{S} \right)_{\text{ox}} \left(\frac{1}{f_{\text{ox}}} - 1 \right)$$

$$\overline{\text{PS}} \equiv \overline{Z} = 4 \left(\frac{V}{S} \right)_{\text{ox}}$$

where

$$\left(\frac{V}{S} \right)_{\text{ox}} = \frac{2Na}{La} \quad \text{total volume-to-surface ratio of dispersoid phase}$$

Na number of intercepts of random traversing line(s) with boundaries of dispersoid phase

f_{ox} volume fraction of secondary phase particles

No attempt was made to calculate \overline{PS} and \overline{IPS} for the Al_2O_3 particles in the extraction-replication and thin-film samples because of the virtual impossibility of adequately defining individual platelets.

RESULTS

Surface Replication

These results are shown in figure 1 for $Al + Al_2O_3$ and in figure 2 for $Ni + ThO_2$. The $Al + Al_2O_3$ has many relatively large platelets. Some smaller spherical particles also appear. The $Ni + ThO_2$ has fairly uniformly distributed spheroidal particles.

Extraction Replication

These results are shown in figure 3 for $Al + Al_2O_3$ and in figure 4 for $Ni + ThO_2$ materials. In the former, the particles appear as flakes; in the latter, the particles appear spheroidal. Comparison of figures 1 and 3 suggests that the volume percent and \overline{PS} of the Al_2O_3 particle are greater when based on extraction replication than when based on surface replication. Volume percent and \overline{PS} appear similar for the $Ni + ThO_2$ whether based on surface or extraction replication (compare figs. 2 and 4). The definition of some of the larger individual platelet particles in the extraction replication, comparing figures 1 and 3, is fairly good, but in the case of the smaller and also the larger aggregated particles, the delineation of particles is poor. The definition of the ThO_2 particles as indicated in the extraction electron photomicrograph (fig. 4) is generally good except for overlapping particles or some of the very fine particles.

Thin Films

The electron photomicrograph of a thin film of $Al + Al_2O_3$ (fig. 5) suggests that the dispersoid is present as flakes but does not allow delineation of individual particles, because of clustering. An electron photomicrograph of a thin film of $Ni + ThO_2$ (fig. 6) suggests that the ThO_2 is present as spheroids (the other two methods also suggest this). Inspection of these figures indicates an apparently larger volume percent dispersoid and a smaller \overline{IPS} than do the corresponding surface-replication electron photomicrographs.

Figures 7 and 8 show a stereoscopic effect if a stereo-viewer is used. In the absence of such a viewer, a three-dimensional effect may be obtained by placing a card or a piece of paper vertically between the eyes and sighting on the two mating micrographs. Adjusting the distance between the eyes and the micrographs can give a three-dimensional effect. Then figure 7 shows that the Al_2O_3 consists of rolled, curled, and twisted platelets many of which appear to be aggregated. Many of the platelets evidently form tubes or cylinders. There seem to be few, if any, small spherical particles. The $\text{Ni} + \text{ThO}_2$ contains fairly uniformly distributed and distinct spheroidal thoria particles (fig. 8). Variation in matrix thickness can make it difficult to define some particles. This is because electron-beam transmission is affected by local film thickness and can thus cause ripples in the electron photomicrographs (fig. 5).

Comparison of Parameters Obtained for Different Methods Studied

Reference to table I, which contains a summary of particle parameters (i. e., volume percent, $\overline{\text{PS}}$, $\overline{\text{IPS}}$, and minimum particle size), shows best agreement between nominal and measured volume percent dispersoid when using surface replication for either material. For $\text{Al} + \text{Al}_2\text{O}_3$, the amount of dispersoid progressively increased from replication to extraction to the thin-film method; these last two methods gave volume percent values of Al_2O_3 that were about 7 times greater than those given by the replication method. For the $\text{Ni} + \text{ThO}_2$, the volume percent of dispersoid as determined from the extraction replica was slightly greater than that obtained from the surface replica; however, the value of volume percent dispersoid obtained from the thin film was about 6 times the nominal value. The values of $\overline{\text{PS}}$ and $\overline{\text{IPS}}$ determined for the $\text{Ni} + \text{ThO}_2$ were essentially the same whether determined from replication or extraction micrographs; the value of $\overline{\text{IPS}}$ based on the thin film, however, was substantially less than that yielded by the former two methods. No attempt was made to determine $\overline{\text{PS}}$ and $\overline{\text{IPS}}$ for Al_2O_3 by extraction or thin film because it was virtually impossible to delineate individual particles.

In all instances, the finest particle dimensions observed with a calibrated $3\times$ eyepiece were estimated to be about 100 \AA ($0.01 \mu\text{m}$). It should not be inferred that this value represents the limit of resolution of any of the three methods.

The dimensions of the photomicrographs, their magnifications, and the numbers of particles counted for the $\text{Ni} + \text{ThO}_2$ are as follows:

Method	Magnification	Photomicrograph size, in. (cm)	Number of parti- cles counted
Surface replication	×49 000	7 × 9 (17.8 × 22.9)	217
Extraction replication	×49 000	7 × 9 (17.8 × 22.9)	189
Thin film	×49 000	^a 7 × 9 (17.8 × 22.9)	388

^aActual area used for counting was $2\frac{3}{4} \times 3\frac{1}{4}$ in. (6.9 × 8.1 cm).

DISCUSSION

Surface Replication

Surface replication gave the closest agreement with the corresponding nominal amounts of oxide. For both materials, the finest particle dimension observed was estimated to be 100 Å (10 nm), as mentioned previously.

In surface replication, excessive etching must generally be avoided on any type of specimen to avoid revealing more than one "layer" of particles or "etching out" particles. In materials containing platelets (i. e., Al + Al₂O₃) rather than spheroidal particles, inadvertent excessive etching might reveal too many particles (see fig. 9). It might be noted that an accurate determination of volume percent as well as \overline{PS} and/or \overline{IPS} is predicated upon adequate sampling or the selection of a truly typical section. For the purposes of this study representative sections were selected by viewing a number of specimens obtained from the surface of one piece of each material.

Extraction Replication

Extraction replication yielded a value of volume percent dispersoid for the Ni + ThO₂ slightly higher than nominal; for the Al + Al₂O₃, considerably greater. The slightly greater volume percent ThO₂ could have been a statistical effect. It is believed, however, that some particles were already in a state of aggregation and that others not initially attached to the extraction film were dissolved free of the matrix and became attached to particles already adhering to the extraction film. For the Al + Al₂O₃ platelets, the initial state of aggregation was so great that, upon extraction, many "layers" of oxide were extracted, giving a much higher volume percent of dispersoid than the nominal. The finest extracted ThO₂ or Al₂O₃ particle dimensions observed were of the order of 100 Å (0.01 μm), as with surface replication.

Ashby and Ebeling (ref. 7) have proposed using extraction replicas to determine

volume percent, \overline{PS} , and \overline{IPS} and have derived equations to yield these values for spherical dispersoids. Their method can certainly be used to calculate \overline{PS} ; but, as they point out, volume percent and \overline{IPS} depend on extraction efficiency. If this is less than 100 percent, the volume percent will be too low and \overline{IPS} (an inverse function of volume percent) too high. Conversely, if the dispersoid particles are aggregated, extraction efficiency could exceed 100 percent; the calculated volume percent would then be high, \overline{IPS} low. Ashby and Ebeling's results with copper and silica ($Cu + SiO_2$) indicated that the extracted SiO_2 varied from about 50 to 100 percent of the incorporated amount.

Thin-Film Microscopy

The thin-film method gave considerably greater volume fractions of dispersoid compared to their respective nominals for the two materials. This is probably because the films contain many "layers" of oxide. However, an exceedingly thin film, approaching a monolayer of oxide, presents another problem: particles may fall out as illustrated schematically in figure 10.

For $Ni + ThO_2$, the low \overline{IPS} ($0.28 \mu m$) calculated from the measurements and the high volume percent (11.9 percent) are indicative of the problem of measuring the underlying particles in the three-dimensional specimen.

Stereographs of thin films give excellent pictures of layering and of the spatial relations and shapes of particles.

Comparison of the Methods

Table II gives the a priori and experimentally determined advantages and disadvantages of the three methods.

A question arises whether the surface replication method, which seems experimentally and inductively the most accurate when used with a topological analysis, retains the true distribution of particles. It may, conceivably, not reveal all the finer ones. To permit a comparison, normalized (figs. 11 to 13) and cumulative (fig. 14) frequency distribution curves were plotted for the $Ni + ThO_2$ material. Areas with apparently typical distributions and without excessive particle overlap were carefully selected. The distributions (based on the use of the Zeiss particle-size analyzer) are essentially similar for surface replication, extraction replication, and thin film. It should be expected that the frequency-distribution curve obtained for the thin film (from a typical area relatively free of particle overlap) would be the most definitive, particularly for the finer particles. We should expect the finer particles to be retained more surely and to be better delineated

than with the replication methods, where artifacts and matrix effects may cause ambiguities (compare figs. 2, 4, and 6). These results suggest that, at least in the case of the Ni + ThO₂, the particle size distribution was essentially preserved by the use of either surface or extraction replication and that the fine particles were retained.

Recommendations for Characterization of Dispersoids

When the microstructural parameters of volume percent, \overline{PS} , and \overline{IPS} are determined by quantitative metallography, the results are considered most accurate when based on surface replication, provided that the great majority of particles can be resolved. Even if some of the finer particles could not be resolved, they would probably have slight effect on the calculated values of volume percent and \overline{PS} .

Extraction replication gives good definition of discrete particles. In cases where matrix effects obscure the finer particles, or minor porosity prevents good etching results, extraction methods offer an alternative that can represent planar sections fairly well and thus give good values for the microstructural parameters. Extraction films, too, may be examined by electron and X-ray diffraction. Sometimes, as noted previously, it is difficult to differentiate between a very fine particle, artifact or a matrix effect. Thin films or extraction replicas may then help to reveal the fine particles and thus permit more reliable measurements to be made from the surface replicas. The thin-film method permits a stereoscopic view of spatial distribution and helps to determine particle geometry. In general, the methods complement each other. Surface replication has a very practical advantage: it can be used with partially densified (i. e., porous) dispersion-strengthened materials. There are numerous occasions involving partially densified dispersion-strengthened materials where the use of electron microscopy might be advantageous for the estimation of particle size and spacing. The examination of cold compacted specimens (ref. 8) to determine particle size and distribution prior to sintering or further processing exemplifies the use of such partially densified materials.

CONCLUSIONS

The results of this investigation of the relative merits of surface replication, extraction replication, and thin-film methods currently used at Lewis to characterize dispersoids of different geometries and spatial relations and with about 100 Å (0.01 μm) finest observed dimensions lead to the following conclusions:

1. Surface replication gave the best agreement of measured and nominal amounts of oxide, whether the particles were discrete spheroids or aggregated platelets. This

method also seemed to yield the most satisfactory values of \overline{PS} and \overline{IPS} .

2. Extraction replication was satisfactory for the material containing discrete spheroidal particles ($Ni + ThO_2$) in that it also gave satisfactory agreement between measured and nominal amounts of oxide and also helped define the size and presence of fine particles. The values of \overline{PS} and \overline{IPS} were also felt to be satisfactory. This method was not considered adequate for the material containing platelets ($Al + Al_2O_3$); the oxide volume percent was considerably in excess of the nominal value and, because of the virtual impossibility of differentiating individual particles, it did not appear possible to calculate meaningful values of \overline{PS} and \overline{IPS} . The results obtained by this method seemed to depend on the type of dispersoid, its state of aggregation, and the effectiveness of the extraction technique.

3. The thin-film method, while helping to verify the presence of the finer particles, gave considerably greater volume fractions of dispersoids compared to their corresponding nominal amounts for the two materials. With $Ni + ThO_2$, the calculated \overline{IPS} decreased; with $Al + Al_2O_3$, even an apparent \overline{PS} or \overline{IPS} could not be determined because of particle aggregation and/or overlap.

4. The particle-size frequency distributions obtained from each method for $Ni + ThO_2$ essentially agreed, suggesting that all three methods would give similar distributions for discrete particles.

5. Stereoscopic viewing of thin-film specimens should permit possible morphology studies to be made involving qualitative observations of particle shapes and spatial relations. Under some circumstances stereoscopic views of thin films can complement surface-replication or extraction-replication results and may be used, at least initially, to cross check the interpretations and results obtained by the other methods.

Lewis Research Center,
National Aeronautics and Space Administration,
Cleveland, Ohio, November 20, 1967,
129-03-01-05-22.

APPENDIX - DERIVATION OF EQUATIONS

Equations (1) and (2) were derived as follows. Equations (1) and (7) of reference 6 are, respectively,

$$\overline{IPS} = 4 \left(\frac{V}{S} \right)_{\text{ox}} \left(\frac{1}{f_{\text{ox}}} - 1 \right) \quad (\text{A1})$$

and

$$\bar{Z}_{\text{ox}} = 4 \left(\frac{V}{S} \right)_{\text{ox}} \quad (\text{A2})$$

In reference 5, equation (4) gives the ratio of perimeter to particle area as

$$\frac{P}{A} = \frac{\pi Na}{2La} \quad (\text{A3})$$

and equation (8) (also of ref. 5) gives the ratio of surface to volume as

$$\frac{S}{V} = \frac{2Na}{La} \quad (\text{A4})$$

where

Na number of intercepts of grid (i. e. , traversing) lines with lines bounding particle phase

La total length of grid (i. e. , traversing) lines intercepted by particle phase

P total particle perimeter

A total particle area

V total particle volume

S total particle surface

Algebraic rearrangement of (A3) and (A4) gives

$$\frac{A}{P} = \frac{4}{\pi} \times \frac{V}{S}$$

Hence, substituting A/P for V/S in equations (A1) and (A2) gives the following relations:

$$\overline{IPS} = \pi \left(\frac{A}{P} \right)_{\text{ox}} \left(\frac{1}{f_{\text{ox}}} - 1 \right)$$

$$\overline{PS} \equiv \overline{Z} = \pi \left(\frac{A}{P} \right)_{\text{ox}}$$

REFERENCES

1. Hoffman, Charles A.; and Weeton, John W.: Metallographic Study of Dispersion-Strengthened Alloys After Failure in Stress Rupture. NASA TN D-3527, 1966.
2. McKinney, C. D.; and Tarpley, W. B.: Aerosol Preparation of Composite Metal Powders for Dispersion Strengthening. Rep. No. RR-61-30, Aeroprojects, Inc., Mar. 1961.
3. Peiffer, Howard R.: The Effect of Microstructure on the Properties of Dispersion Hardened Materials. Final Tech. Rep. (Contract NOa(s) 59-6230-C), RIAS, Inc., Oct. 1960.
4. Bloch, E. A.: Dispersion-Strengthened Aluminum Alloys. Met. Rev., vol. 6, no. 22, 1961, pp. 193-239.
5. Smith, Cyril S.; and Guttman, Lester: Measurement of Internal Boundaries in Three Dimensional Structures by Random Sectioning. Trans. AIME, J. Metals, vol. 197, no. 1, Jan. 1953, pp. 81-87.
6. Cremens, W. S.: Use of Submicron Metal and Nonmetal Powders for Dispersion-Strengthened Alloys. Ultra Fine Particles. W. E. Kuhn, ed., John Wiley and Sons, Inc., 1963, pp. 457-478.
7. Ashby, M. F.; and Ebeling, R.: On the Determination of the Number, Size, Spacing, and Volume Fraction of Spherical Second-Phase Particles from Extraction Replicas. Trans. AIME, vol. 236, no. 10, Oct. 1966, pp. 1396-1404.
8. Reinhardt, Gustav; Cremens, Walter S.; and Weeton, John W.: Cold Consolidation of Metal Plus Dispersoid Blends for Examination by Electron Microscopy. NASA TN D-3511, 1966.

TABLE I. - SUMMARY OF PARTICLE PARAMETERS

[Finest observed particle size was 100 Å (0.01 μm) using a calibrated 3× eyepiece.]

Method	Volume percent	Average particle size, \overline{PS} , μm	Average interparticle spacing, \overline{IPS} , μm
Al + 5 percent Al ₂ O ₃			
Surface replication	6.8	0.13	1.8
Extraction replication	47	(a)	(a)
Thin film	52	(a)	(a)
Ni + 2 percent ThO ₂			
Surface replication	1.9	0.04	1.9
Extraction replication	2.4	.05	2.0
Thin film	11.9	.04	.28

^aCould not delineate individual particles, hence could not meaningfully calculate \overline{PS} and \overline{IPS} .

TABLE II. - COMPARISON OF ELECTRON MICROSCOPY METHODS

Method	Advantages		Disadvantages	
	A priori	Experimental	A priori	Experimental
Surface replication	Simple and rapid; good approximation to plane surface - hence, amenable to topological analysis. Can be used with partially densified material.	Gives some indication of particle shapes. Good agreement with nominal amounts of oxide.	May have higher threshold resolution than other two methods.	Prone to artifacts and matrix effects.
Extraction replication	May give sufficiently planar section for topological analysis. Good definition of all particles. Can be used with partially densified material.	Good definition of larger particles. Good agreement with nominal amount of oxide, with essentially discrete particles.	With aggregated particles, may result in extraction of particle "layers." Particles may shift, be "lost," or be entirely dissolved. Dissolution of matrix may form new compounds.	May be difficult to interpret in the case of very fine particles. Some particles may overlap.
Thin film	Good definition of all particles provided that overlapping is minimal. Excellent for qualitative and morphological studies when view is stereoscopic.	Good definition of fine as well as large particles. Good definition of particle shape and distribution, when view is stereoscopic.	Not amenable to topological analysis unless film is very thin; then large particles may fall out. Not adaptable to highly porous materials.	Can lead to greatest errors in determining volume percent, \overline{PS} , and \overline{IPS} of dispersoid.

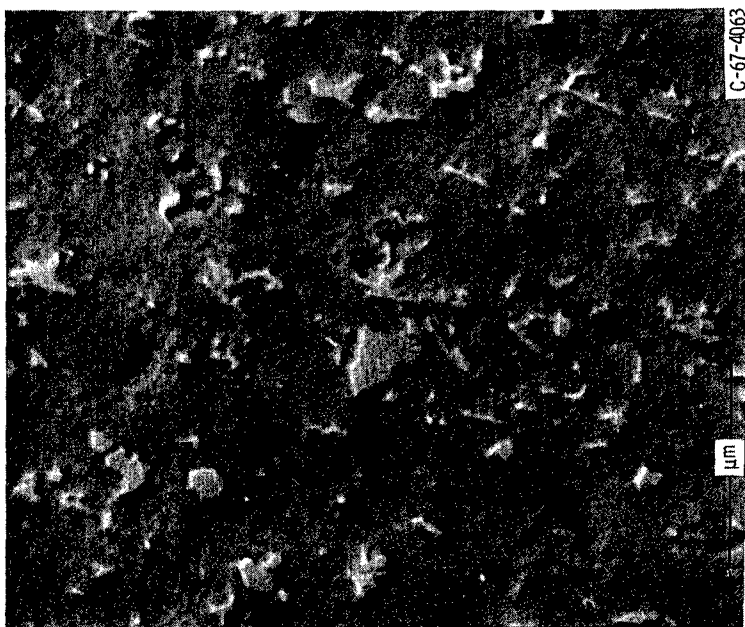


Figure 1. - Microstructure of Al + Al₂O₃ obtained by surface replication.
X28 300.

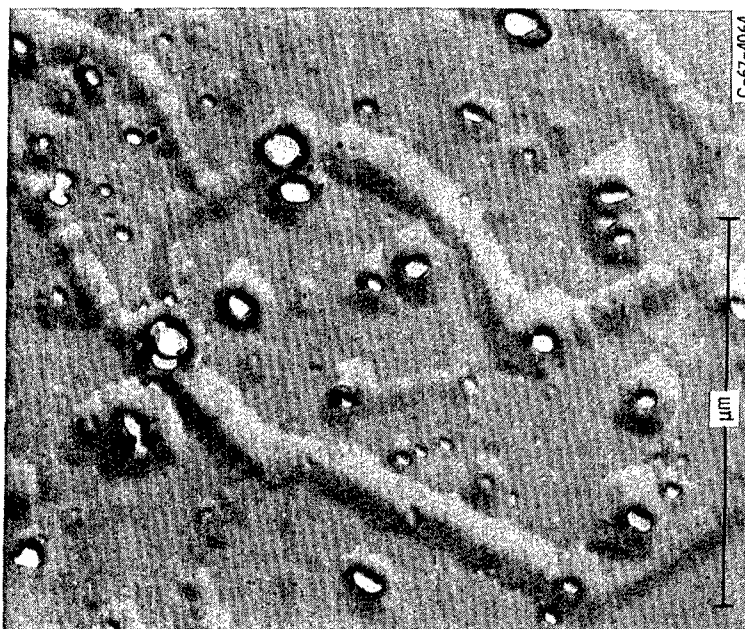


Figure 2. - Microstructure of Ni + ThO₂ obtained by surface replication.
X49 000.

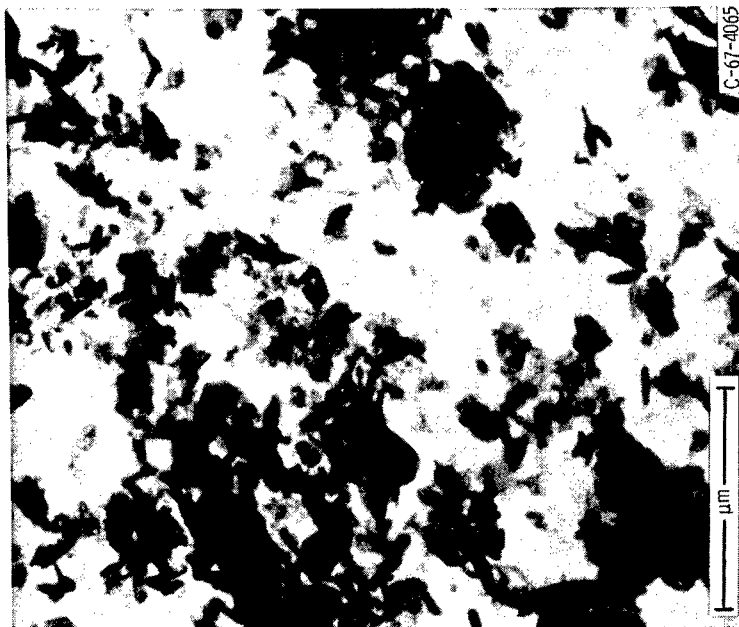


Figure 3. - Microstructure of Al + 5 Al₂O₃ obtained by extraction replication. X28 300.

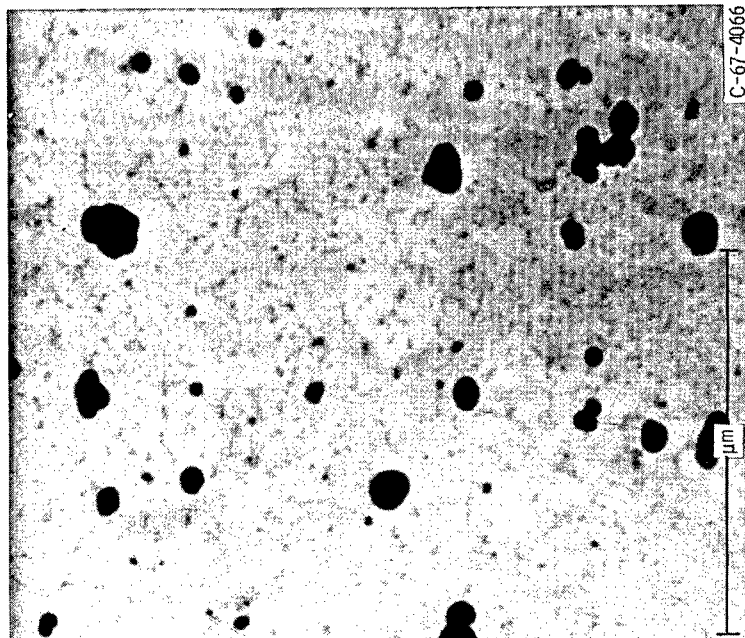


Figure 4. - Microstructure of Ni + ThO₂ obtained by extraction replication. X49 000.

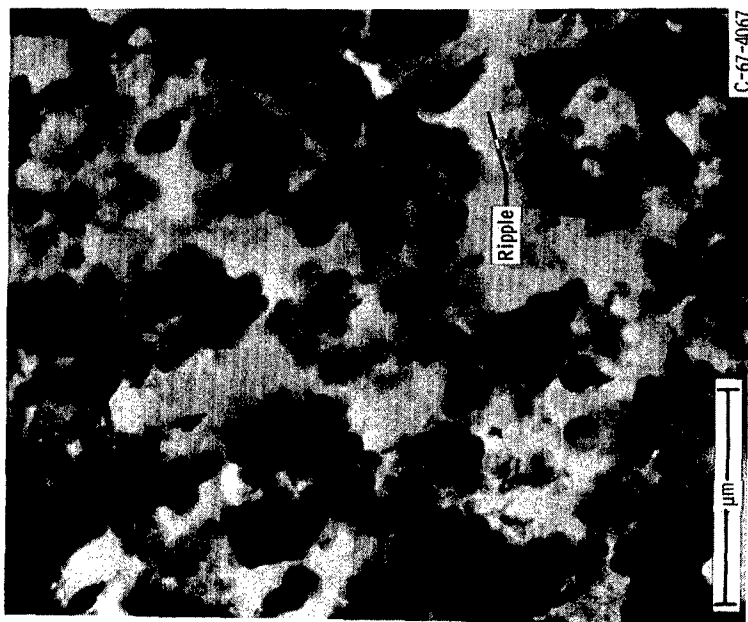


Figure 5. - Microstructure of Al + Al₂O₃ obtained by thin-film method. X27 000.

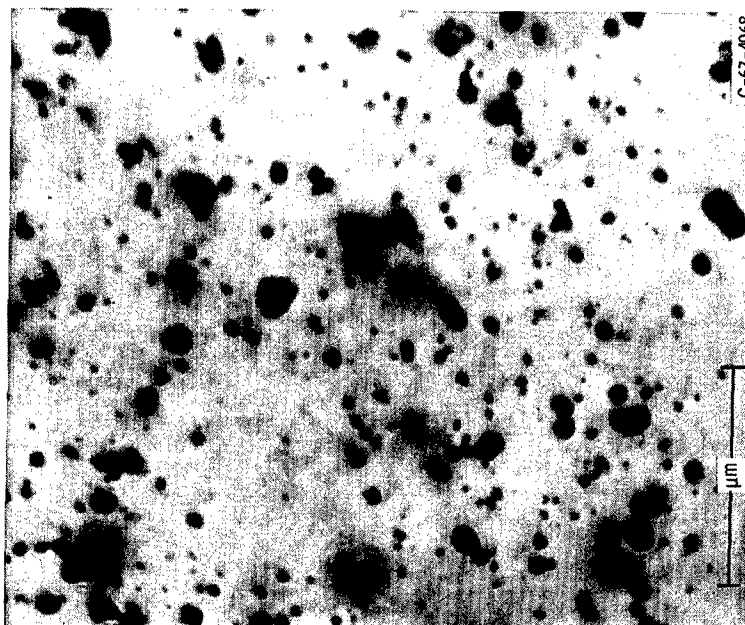


Figure 6. - Microstructure of Ni + ThO₂ obtained by thin-film method. X49 000.



Figure 8. - Stereo thin-film micrograph of Ni + ThO₂. X28 000.

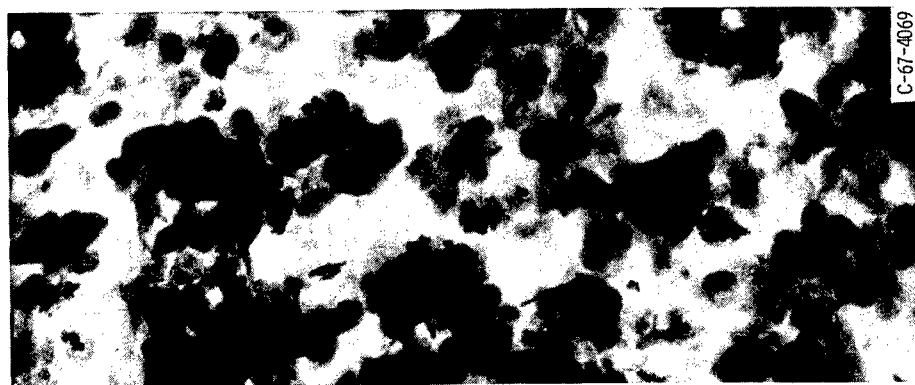
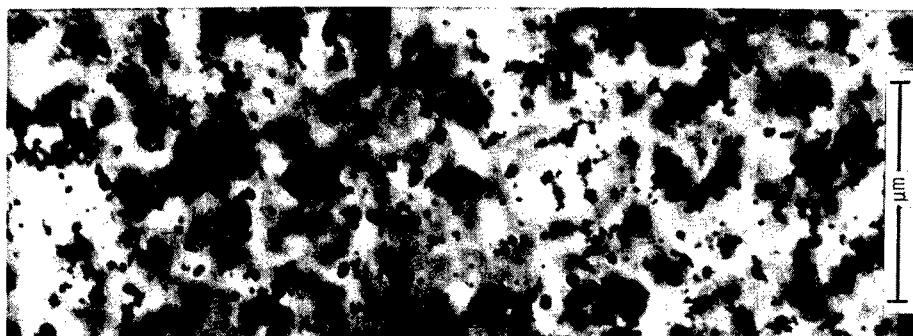
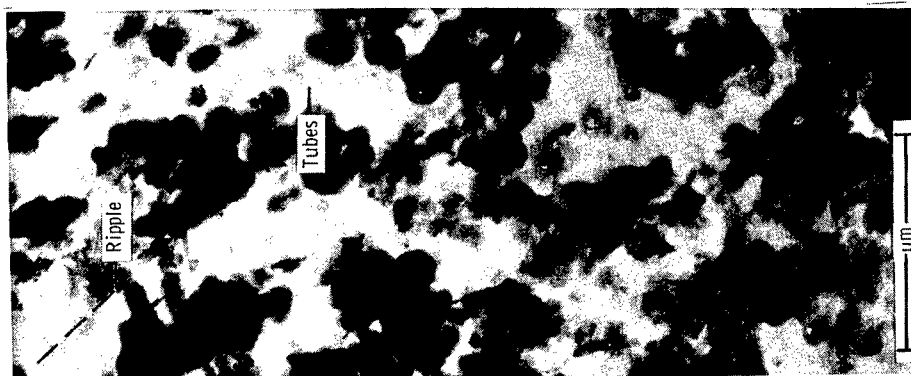


Figure 7. - Stereo thin-film micrographs of Al + Al₂O₃. X27 000.



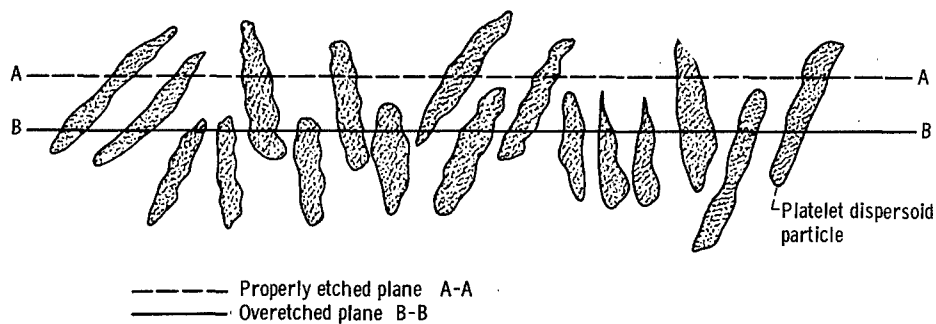


Figure 9. - Schematic illustration of effects of overetching.

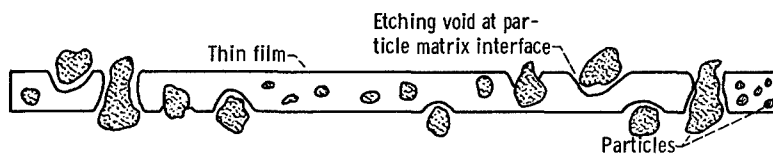


Figure 10. - Schematic illustration of mechanism of loss of large particles from excessively thinned film.

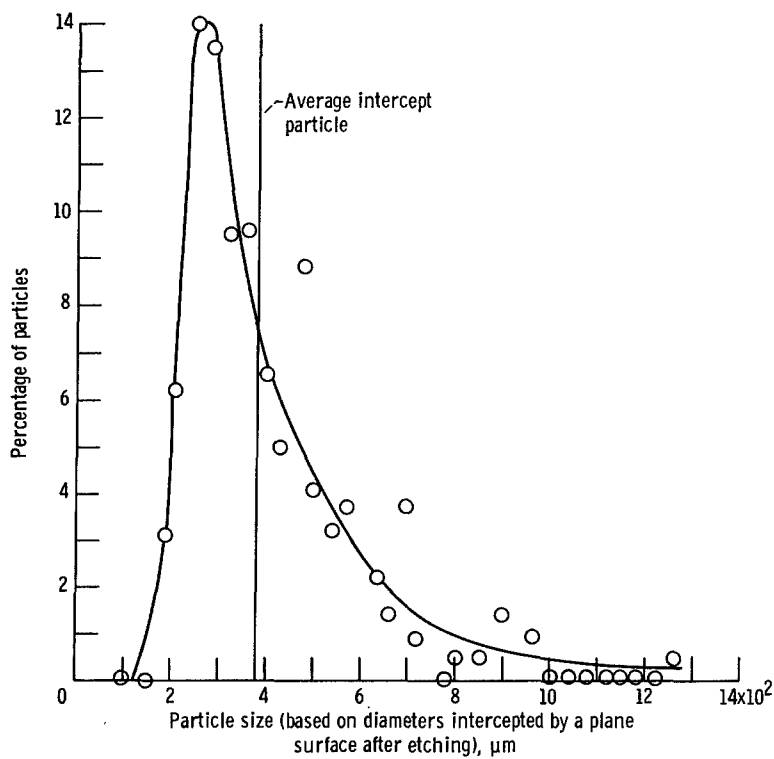


Figure 11. - Normalized particle size distribution based on surface replication - Ni + ThO₂. Zeiss particle-size analyzer used; number of particles counted, 217; size of micrograph, 7 by 9 inches (17.8 by 22.9 cm). X49 000.

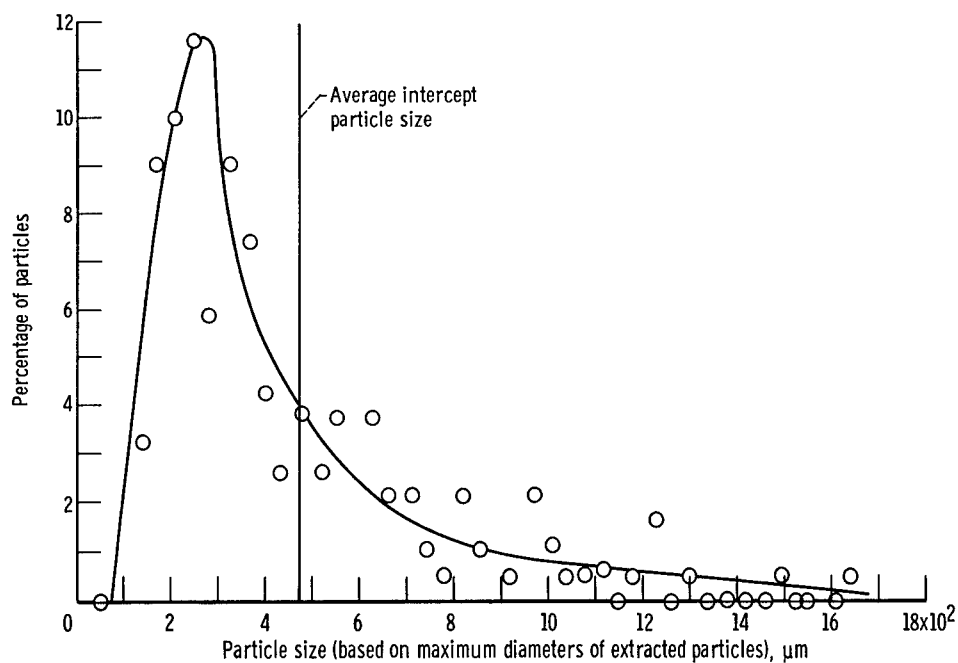


Figure 12. - Normalized particle size distribution based on extraction replication - Ni + ThO₂. Zeiss particle-size analyzer used; number of particles counted, 189; size of photomicrograph, 7 by 9 inches (17.8 by 22.9 cm). X49 000.

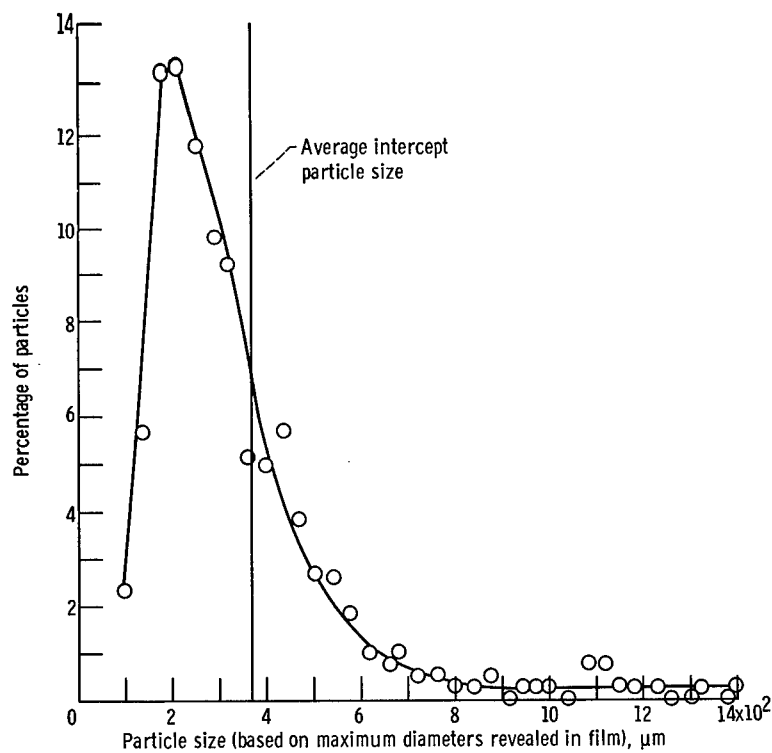


Figure 13. - Normalized particle size distribution based on thin film - Ni + ThO₂. Zeiss particle-size analyzer used; number of particles counted, 388; size of photomicrograph, 2 $\frac{3}{4}$ by 3 $\frac{1}{4}$ inches (6.9 by 8.1 cm). X49 000.

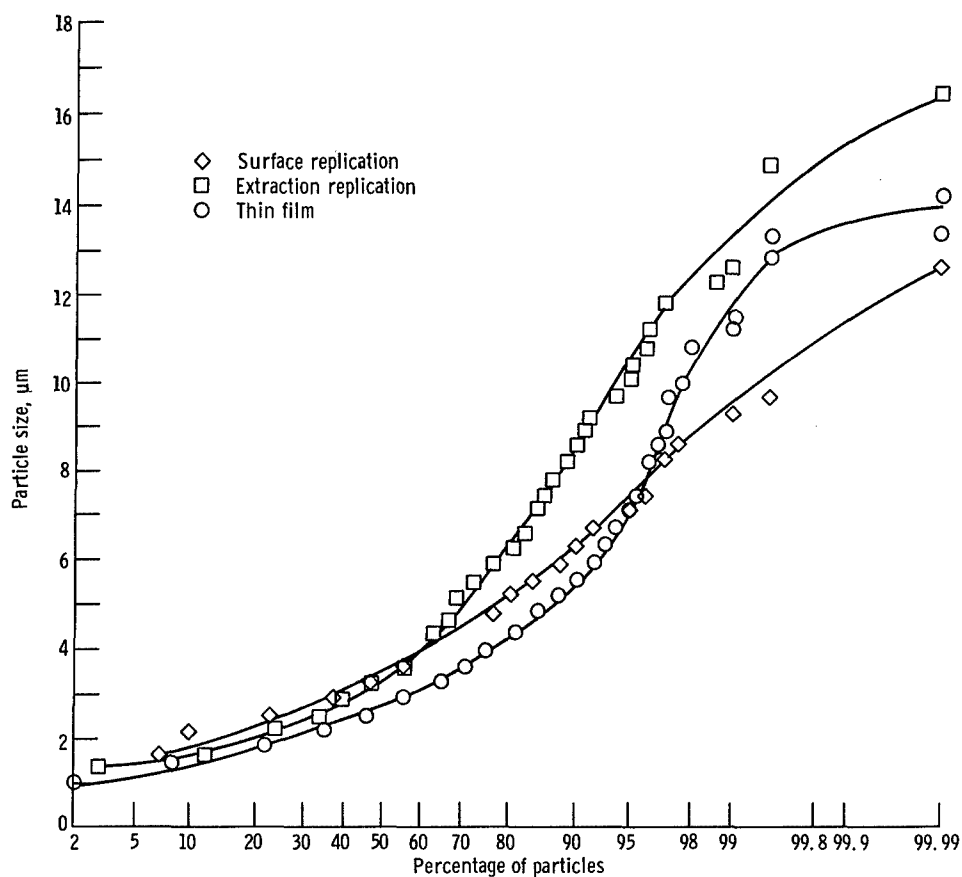


Figure 14. - Cumulative distribution of particle sizes obtained from surface replication, extraction replication, and thin-film methods for $\text{Ni} + \text{ThO}_2$.